ISSN: 2414-1895 DOI: 10.6919/ICJE.202301_9(1).0006

Machine Vision Detection System for the Tenon Size of Aero-engine Blades

Tian Yang[1], Qinyuan Huang[1, 2], Jiarui Luo[1], Ying Zhou[1]

[1] Sichuan University of Science & Engineering, School of Automation and Information Engineering, Zigong 643002, China

[2] Artificial Intelligence Key Laboratory of Sichuan Province, Zigong 643002, China

Abstract

Given the problems of low efficiency in the manual detection process of aero-engine blade tenon and difficulty in meeting batch detection, this paper designed a machine vision detection system for the tenon size of aero-engine blades. Firstly, the image acquisition device of the blade tenon is built. Secondly, an adaptive bilateral filter Canny operator is designed for contour edge detection. At the same time, to improve the positioning accuracy of lines and circles, an edge-fitting algorithm combining Hough transform and least squares are proposed to measure lines and circles. Finally, according to the geometric calculation, the machining size error of the tenon is obtained, and whether the tenon contour size is qualified is judged. Experiments have verified that the method has high dimensional detection accuracy and fast execution efficiency. The average length error is less than 0.03mm, and the angle error is 0.056 degrees. Compared with the traditional method, it is more suitable to meet the contour size detection requirements of an aero-engine blade tenon.

Keywords

Aero-engine Blade; Tenon; Edge Fitting.

1. Introduction

The blade is an essential part of the aero-engine, composed of the blade body and tenon [1,2]. The blade is fixed on the engine through the fitting of tenon and mortise. If the tenon size is unqualified, there may be a risk of failure to fit or falling off. The current traditional tenon size detection method is the enlarged projection method. The judgment is made by visually observing and comparing the measured tenon profile and the standard tenon profile under the enlarged projection. As the demand for qualified blades continues to expand, the traditional detection method is no longer applicable, and the rapid detection of the tenon size has become an urgent problem to be solved.

Machine vision technology [3], which simulates human visual function through digital image processing, has been widely used in size detection [4]. With its non-contact and digital characteristics, it can significantly improve the execution efficiency of reviews. Ngoc Vu Ngo et al. used a three-dimensional measurement system to obtain its feature points in the world coordinate system to calculate the measurement data [5]. Junhui Huang et al. hole radius and spacing measurement method is presented based on binocular vision combined with dynamic local plane for the large-size workpiece with plane feature [6]. Jia L put forward an Image feature recognition method based on the Hough transform, and the size detection algorithm is designed on this basis [7].

Through previous studies, it can be found that using the Canny[8,9] operator and curve fitting helps detect various edge cases; Profile detection can be done by edge detection, which has the potential to realize the dimension detection of blade tenons. However, there is still much room for improvement

ISSN: 2414-1895 DOI: 10.6919/ICJE.202301_9(1).0006

in the detection accuracy of the current method. Therefore, in this paper, a machine vision detection system for blade tenon size is designed. The detection platform collects the image of the tenon and obtains the detection results according to the corresponding detection algorithm designed. The detection algorithm is particularly critical. First, accurate edge features are obtained based on improved bilateral filtering adaptive Canny operator, and then edge curves are fitted by combining Hough detection and least squares. Finally, the calculation and detection of tenon size are completed.

2. Detection System Design

The detection system mainly includes two parts: hardware system and software algorithm. The hardware system is used to obtain clear and reliable blade tenon images and save the images to the computing storage unit; the software is used primarily to complete image analysis and output detection results.

2.1 Hardware Structure

The blade tenon of an aero-engine is shown in Fig. 1(a), which adopts the most widely used fir tree structure in turbines. The two ends are in the shape of a giant wedge and a small wedge. The wedge shape occupies a smaller circumferential dimension on the wheel rim, so more blades can be installed. The blades are also easy to disassemble and replace. There are symmetrically distributed semicircular mortise teeth on both sides of the mortise, which can fit with the inverted wedge-shaped mortise and groove of the same profile on the wheel rim.

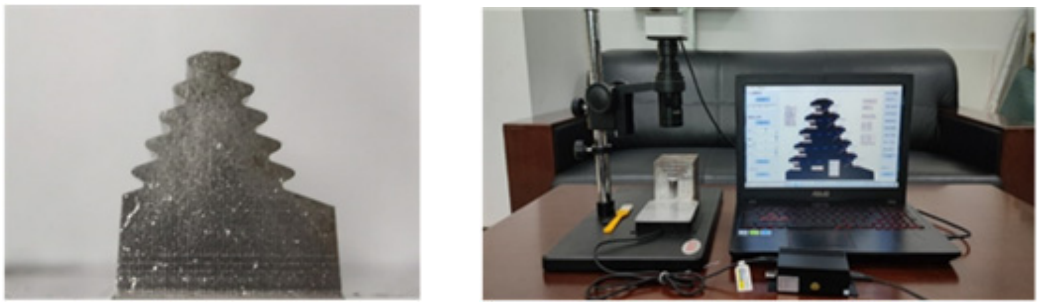

(a) blade tenon (b) Image acquisition device

Figure 1. Detection system hardware

The image acquisition device of the blade tenon is shown in Figure 1(b), which consists of a camera, a lens, a light source, and a computer. The camera adopts the Newhall company model DZ-9288 industrial camera; the camera resolution is 4000*3000. In addition to the camera, a suitable light source type and lighting method are conducive to acquiring high-quality images. Compared with top-light ring lighting, parallel backlight lighting can produce images with sharp edges and fewer transition pixels at the border. Therefore, the lighting method adopts Parallel backlighting for sharp-edge images.

2.2 System Software Structure

The processing after image acquisition needs to be completed by the software system. This research uses Python language and Opencv library Design and implements related algorithms, and the detection algorithm flow of the blade tenon is shown in Figure 2.

Algorithm flow: First, grayscale the collected image of the tenon; use the adaptive edge operator of bilateral filtering to extract the edge pixels of the tenon; use the Hough transform to detect the straight line in the edge initially, and segment and filter the edge points; Then use the least square method to fit precise straight lines and circles; finally calculate the dimensions of each part of the tenon according to the geometric relationship.

ISSN: 2414-1895 DOI: 10.6919/ICJE.202301_9(1).0006

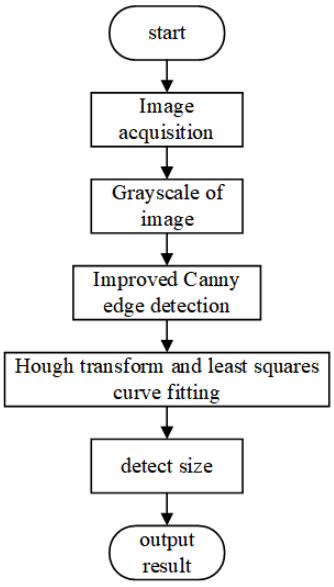

Figure 2. Detection algorithm flow

3. The Key Algorithm of Blade Tenon Detection

3.1 Improved Edge Detection

Bilateral filtering is developed based on Gaussian filtering[10]. When sampling, the spatial distance of pixels is considered, and the grey similarity of pixels is added. Compared with Gaussian filtering, this combination of spatial proximity and The weighted processing of the parallel with the grey value can make the filter kernel change non-linearly according to different grey values at different positions in the image. This weighted method, which considers spatial information and grey similarity simultaneously, achieves the purpose of edge preservation and denoising and has the characteristics of simple, non-iterative, and local processing. Therefore, the effect of maintaining edges and smoothing noise reduction can be achieved. The bilateral filtering formula is as follows:

$$\bar{I}(p) = \frac{1}{W_p}\sum_{q\in S} G_{\sigma_s}(\|p-q\|)G_{\sigma_r}(|I(p)-I(q)|)I(q) \tag{1}$$

$$W_p = \sum_{q\in S} G_{\sigma_s}(\|p-q\|)G_{\sigma_r}(|I(p)-I(q)|) \tag{2}$$

$$G_{\sigma_s}(\|p-q\|) = e^{-\frac{(i-m)^2+(j-n)^2}{2\sigma_s^2}} \tag{3}$$

$$G_{\sigma_r}(|I(p)-I(q)|) = e^{-\frac{[I(i,j)-I(m,n)]^2}{2\sigma_r^2}} \tag{4}$$

q represents the adjacent pixel, The (m,n) represents the coordinates of the adjacent pixel, $I(m,n)$ represents the value of the adjacent pixel, p represents the central pixel, (i,j) the coordinates of the central pixel, $I(i,j)$ represents the value of the centre pixel. G_{σ_s} calculates the space domain, G_{σ_r} calculates the pixel domain and traverses each image pixel to obtain the filtering result.

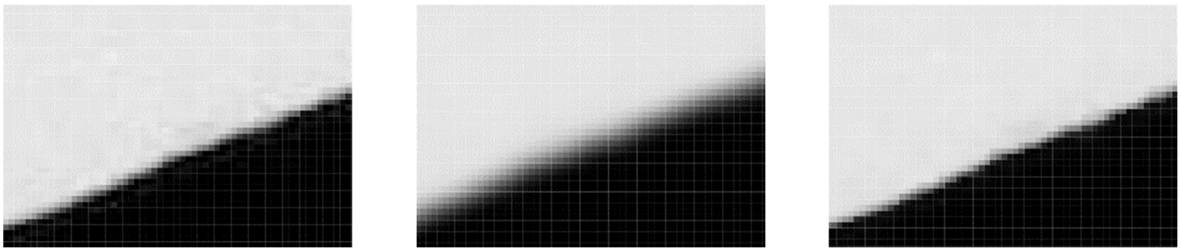

(a) Original picture details (b) Gaussian filter (d) Bilateral filter

Figure 3. Filtering effect of blade tenon image

ISSN: 2414-1895 DOI: 10.6919/ICJE.202301_9(1).0006

The filtering effects of Sissian and bilateral filtering are shown in Figure 3. Although the noise is eliminated after Gaussian filtering, the edge part of the image is blurred to a certain extent, which has a particular impact on the edge extraction. The bilateral filtering algorithm preserves the edge contour well while removing the image noise, so this paper replaces the Gaussian filtering in the traditional Canny algorithm with bilateral filtering.

The maximum between-class variance method is based on the grey histogram information of the image to complete the threshold selection automatically. Assuming a target image with a size of $M \times M$, the grey value range is $[0, L-1]$, and the pixels whose grey value is less than t in the image are classified into a class $C0$, that is, $[0, t] \in C0$, and the rest The pixels are organized into a class $C1$, that is, $[t+1, L-1] \in C1$, the formula is as follows:

$$P_0(t) = \sum_{i=1}^{t} P_i \tag{5}$$

$$P_1(t) = \sum_{i=t+1}^{L-1} P_i = 1 - P_0(t) \tag{6}$$

$$u_0(t) = \sum_{i=0}^{t} \left(i \frac{P_i}{P_0(t)} \right) \tag{7}$$

$$u_1(t) = \sum_{i=t+1}^{L-1} \left(i \frac{P_i}{P_0(t)} \right) \tag{8}$$

In the formula, i represents the grey value, P_i is the probability of occurrence of grey value i, $P_0(t)$, $P_1(t)$ represent the probability of occurrence of categories $C0$ and $C1$, respectively, $u_0(t)$, $u_1(t)$ represent the probability of category $C0$, the average grey level of $C1$. According to the above results, the inter-class variance expression of the image can be obtained as follows:

$$\sigma(t) = P_0(t)u_0^2(t) + P_1(t)u_1^2(t) \tag{9}$$

The segmentation threshold when the inter-class variance is the largest is taken as the high threshold T_h, and the low threshold is T_l=T_h/2

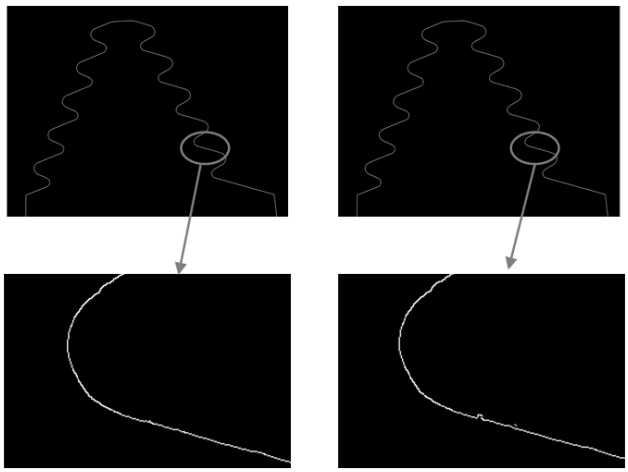

(a) Improved Canny (b) Canny

Figure 4. Canny improved before and after the effect comparison

The maximum inter-class variance method obtains the adaptive threshold, which can avoid the traditional manual setting and adapt well to different light environments, enhancing the algorithm's robustness and providing a good foundation for subsequent size detection.

The effect of edge detection is shown in Figure 4. It can be seen that the improved Canny has a stronger edge-preserving and denoising ability, which makes the extracted edge more complete and can detect the weak edge of the image. The evaluation methods of edge detection are as follows:

$$P = \frac{TP}{TP+FP} \tag{10}$$

$$R = \frac{TP}{TP+FN} \tag{11}$$

ISSN: 2414-1895 DOI: 10.6919/ICJE.202301_9(1).0006

$$F1 = \frac{2*RP}{R+P} \tag{12}$$

Among them, TP represented the number of edge points detected as edge points and marked as edge points; FP represents the number of edge points detected but not marked as edge points; FN represents the number of detected edge points but marked as edge points. The edge detection results before and after improvement are shown in Table 1. It can be seen from the table that the improved algorithm has a better detection effect.

Table 1. Edge detection performance index comparison

Algorithm	P	R	$F1$
Canny	0.8905	0.9062	0.8983
Improved Canny	0.9137	0.9229	0.9183

3.2 Edge Fitting Method Combining Least Square Method and Hough Transform

The overall profile of the tenon is obtained through edge extraction. The shape features are mainly composed of straight lines and arcs. The straight line only needs the slope and intercept, and the circle needs the radius and position. Therefore, the profile data of the tenon needs to be divided. It is the part corresponding to each primitive, which can reduce the amount of data processed and be more accurate in the fitting process of primitives.

The least square method is commonly used for function fitting in mathematical calculations [11]. The principle is to find the best fitting function by minimizing the sum of squared errors of all data points. The formula is as follows:

$$\sum_{i=1}^{N}[y_i - \varphi(x_i)]^2 = S_{min} \tag{13}$$

In the formula (x_i, y_i) represents the data coordinates, $\varphi(*)$ represents the fitted function, and S_{min} represents the sum of squares of the minimized error. The function can be easily obtained by the method of least squares when the data points are known.

Hough transform is a commonly used line detection method in image processing [12]. It has a strong anti-interference ability and is insensitive to incomplete parts, noise and other coexisting non-linear structures in the line. In the Cartesian coordinate system, a line can be determined by the parameter slope and intercept representation. For the Hough transform, the polar coordinate system (ρ, θ) is used to represent the straight line, so the expression of the straight line can be:

$$y = \left(-\frac{\cos\theta}{\sin\theta}\right)x + \left(\frac{\rho}{\sin\theta}\right) \tag{14}$$

Simplification gives:

$$\rho = x\cos\theta + y\sin\theta, \ \ \rho \geq 0, 2\pi > \theta \geq 0 \tag{15}$$

In the formula, ρ represents the distance from the straight line to the coordinate origin, and θ represents the angle between the vertical line and the x-axis. After the straight line transformation in Cartesian coordinates, the parameter space is a family of curves intersecting at one point. This intersection point corresponds to the straight-line parameters in the image to detect the collinearity of feature points in the image. It is a global detection method. And the straight line primitives in the tenon profile curve can be segmented by the method of Hough transform

In theory, a point corresponds to countless straight lines or straight lines in any direction. Still, in actual detection, the number of straight lines (or limited directions) must be limited to be able to calculate, so the direction θ and parameter ρ of the straight line is discretized into finite Discrete values at equal intervals. Then the parameter space is discretized into limited grid units. After transforming the coordinates of each feature point in the image into the parameter space, the obtained value will fall in a certain grid, making the grid unit. The accumulative counter of the unit is increased by 1, and finally, the accumulator exceeds the set value, and then the parameter corresponding to the

ISSN: 2414-1895 DOI: 10.6919/ICJE.202301_9(1).0006

team is a straight-line parameter. Due to the discontinuity of the parameter space, the accuracy of the detection results will be limited by the discrete spacing of the parameters.

Therefore, this study combines the Hough transform and the least square method to fit the geometry of the tenon profile. The method is as follows:

(1) Let the pixel coordinate point set obtained by the edge operator be P, where $P = \{(x_i, y_i)|i = 1,2,\cdots,m\}$, which contains n straight lines, first the pixel coordinate point set P performs Hough transform:

$$\rho_j = x_i \cos\theta_j + y_i \sin\theta_j \ (i = 1,2,\cdots,m;\ j = 1,2,\cdots,n) \tag{16}$$

The parameters (ρ_j, θ_j) of the fitted line can be obtained and rewritten as the oblique intercept formula

$$y_i = a_j x_i + b_j \tag{17}$$

Among them $a_j = -\frac{\cos\theta_j}{\sin\theta_j},\ b_j = \frac{\rho_j}{\sin\theta_j}$

(2) Then calculate the distance from the point in P to the line (a_j, b_j), and set the detection threshold d_k

$$d = \frac{|a_j x_i + b_j - y_i|}{\sqrt{1+a_j^2}}, (x_i, y_i) \in P \tag{18}$$

If $d < d_k$ divide the point (x_i, y_i) into a point set P_j^*, P_j^* represents a point set of a straight line primitive in the image contour and then uses the point set P_j^* as the fitting data, using the least squares method to fit each straight line, the equation of the straight line can be obtained

$$y_i = a_j x_i + b_j \tag{19}$$

(3)After fitting all the straight lines, the remaining points are all arc primitives. Each arc primitive is independent. Randomly select a data point (x_i, y_i) as the starting point, and search 8. The field method finds the data point set S_k^* of the connected region to which the point belongs, then uses the point set S_k^* as the relevant data, and uses the least squares circle fitting method to obtain the circular coordinates and radius of the arc.

Through the Hough transform, each straight line in the contour can be detected, then the connected domain is searched to find the arc segment, and finally, the least squares fitting is performed on each straight line and arc segment, and the fitting result is shown in Figure 5

(a) Original picture details (b) fitting results

Figure 5. Fit of contour

4. Experimental Results

According to the detection requirements, it is necessary to inspect the cross-rod distance, tenon width, tooth shape and wedge angle of the tenon and compare the average result of five detections with the processing design value of the tenon.

(1) Cross-rod distance detection. The rod span is an indirect parameter representing the tooth thickness. Use two measuring rods to clamp in the opposite tooth grooves to measure the size of the outer edge. Generate a virtual measuring rod with a known radius according to the requirements of

ISSN: 2414-1895 DOI: 10.6919/ICJE.202301_9(1).0006

the detection process, make the measuring rod tangent to the two sides of the tooth groove, and then calculate the distance between the centres of the two virtual measuring rods plus the diameter to obtain the distance between the rods:

$$d_A = \sqrt{(x_1 - x_2)^2 + (y_1 - y_2)^2} + 2r_l \quad (20)$$

Among them, $(x_1, y_1), (x_2, y_2)$ are the centre positions of the two virtual measuring sticks respectively, and r_l is the radius of the measuring stick. For each level of tongue and groove detection, the detection results are shown in Table 2.

Table 2. Cross-rod distance detection

Tooth level	True value	Number of detections					Average test results	Error value
		1	2	3	4	5		
1	11.095	11.0738	11.0752	11.0732	11.0746	11.0804	11.07544	-0.01956
2	9.359	9.3434	9.3574	9.3422	9.3485	9.3537	9.34904	-0.00996
3	7.623	7.6098	7.6005	7.6155	7.6024	7.6128	7.6082	-0.0148
4	5.887	5.8796	5.8817	5.8915	5.8818	5.8828	5.88348	-0.00352
5	4.151	4.1437	4.1529	4.1468	4.1425	4.1532	4.14782	-0.00318

Table 3. Tenon width detection

tenon width level	True value	Number of detections					Average test results	Error value
		1	2	3	4	5		
1	9.836	9.8185	9.8153	9.8214	9.8175	9.8196	9.81846	-0.01754
2	8.1	8.0874	8.0912	8.0897	8.0863	8.0887	8.08866	-0.01134
3	6.364	6.3574	6.3594	6.3621	6.3558	6.3592	6.35878	-0.00522
4	4.628	4.6263	4.6351	4.6318	4.6174	4.6155	4.62522	-0.00278
5	2.892	2.8923	2.9152	2.8875	2.8764	2.8971	2.8937	0.0017

Table 4. Detection of the addendum circle radius

Number of circles	True value	Number of detections					Average test results	Error value
		1	2	3	4	5		
1	0.35	0.3288	0.3265	0.3281	0.3275	0.3327	0.32872	-0.02128
2		0.3271	0.3261	0.3284	0.3312	0.3261	0.32778	-0.02222
3		0.3211	0.3235	0.3247	0.3238	0.3284	0.3243	-0.0257
4		0.3269	0.3278	0.324	0.3264	0.3226	0.32554	-0.02446
5		0.3142	0.3258	0.3262	0.3286	0.3189	0.32674	-0.02326
6		0.3220	0.3216	0.3293	0.3274	0.3263	0.32532	-0.02468
7		0.3264	0.3221	0.3237	0.3216	0.3275	0.32426	-0.02574
8		0.3254	0.3284	0.3244	0.3257	0.3243	0.32564	-0.02436
9		0.3211	0.3295	0.3206	0.3248	0.3284	0.32488	-0.02512
10		0.3177	0.3239	0.3221	0.3252	0.3266	0.3231	-0.0269

ISSN: 2414-1895 DOI: 10.6919/ICJE.202301_9(1).0006

(2) The intersection point of the pitch line and the working surface of the tenon is the node, and the distance between the two nodes on the same level tenon is the tenon width. The detection results of the tenon width of each level are in Table 3.

(3) Tooth shape detection: Tooth shape includes the detection of the tooth pitch, addendum circle and dedendum circle of each tenon tooth. The position and radius of the addendum circle and the tooth bottom circle can be directly obtained during the fitting process. The detection results of the addendum circle and the dedendum circle radius are shown in Table 4 and Table 5, respectively. The tooth pitch is calculated by the distance between two adjacent tooth nodes. The detection results are in Table 6.

(4) Wedge angle detection. The wedge angle is the angle between the two pitch lines of the tenon. The wedge angle's size will affect the tenon's bearing capacity. The test results are in Table 7.

Table 5. Detection of the dedendum circle radius

Number of circles	True value	Number of detections					Average test results	Error value
		1	2	3	4	5		
1	0.24	0.2493	0.2453	0.2445	0.2532	0.2431	0.24708	0.00708
2		0.2441	0.2428	0.2462	0.2455	0.2487	0.24546	0.00546
3		0.2494	0.2459	0.2481	0.2476	0.2425	0.2467	0.0067
4		0.2528	0.2498	0.2483	0.2549	0.2514	0.25144	0.01144
5		0.2521	0.2477	0.2472	0.2536	0.2497	0.25006	0.01006
6		0.2373	0.2457	0.2416	0.2382	0.2439	0.24134	0.00134
7		0.2405	0.2462	0.2419	0.2397	0.2428	0.24222	0.00222
8		0.2455	0.247	0.2437	0.2481	0.2406	0.24498	0.00498
9		0.2448	0.2428	0.2442	0.2415	0.2456	0.24378	0.00378
10		0.2385	0.2436	0.2458	0.2396	0.2441	0.24232	0.00232

Table 6. Detection of the tooth pitch

Number of tooth pitch	True value	Number of detections					Average test results	Error value
		1	2	3	4	5		
1	1.98	1.9713	1.9724	1.9716	1.9748	1.9731	1.97264	-0.00736
2		1.9747	1.9738	1.9754	1.9742	1.9722	1.97406	-0.00594
3		1.9773	1.9792	1.9764	1.9758	1.9782	1.97738	-0.00262
4		1.9816	1.9793	1.978	1.9825	1.9767	1.97962	-0.00038
5		1.9764	1.9751	1.9776	1.9759	1.9786	1.97672	-0.00328
6		1.9779	1.9782	1.9827	1.9746	1.9756	1.9778	-0.0022
7		1.9797	1.9763	1.9784	1.9759	1.9808	1.97822	-0.00178
8		1.9793	1.9755	1.9746	1.9771	1.9753	1.97636	-0.00364

In the size detection, the length error of each part of the tenon is less than 0.03mm, and the wedge angle error is 0.056 degrees, which meets the current actual detection needs. In addition, compared

ISSN: 2414-1895 DOI: 10.6919/ICJE.202301_9(1).0006

with traditional manual detection, the visual detection method is more suitable for large-scale, non-contact detection and meets the actual needs of automatic industrial detection.

Table 7. Detection of the wedge angle

Number of wedge angle	True value	Number of detections					Average test results	Error value
		1	2	3	4	5		
8	52	51.95	51.92	51.95	51.96	51.94	51.944	-0.056

5. Conclusion

In order to solve the problem of dimension detection of the tenon of the aero-engine blade, in this paper, a machine vision detection system for the tenon size of aero-engine blades is designed. After the system collects the blade tenon image, the algorithm proposed in this paper is used to measure the overall dimension. In this method, the Gaussian filtering method of the Canny operator is changed to the bilateral filtering method, which retains more edge feature information in the image; at the same time, the maximum inter-class variance method is used to form an adaptive Canny operator threshold, which avoids The artificial setting of the relevant threshold makes the threshold more match the edge features of the image; secondly, the edge fitting method is established by combining Hough transform, and least squares, which solves the problem of low fitting accuracy of Hough transform and least squares Multiplication cannot segment the straight line primitives of the edge, which improves the effect of edge fitting. Compared with traditional methods, our proposed method has higher dimension detection accuracy, more reliable contour dimension detection results, and higher detection execution efficiency.

However, with the gradual increase in the demand for precise detection and accurate detection of aero-engine blade tenons, there is still room for improvement and improvement in the image acquisition quality, edge extraction accuracy, and size detection accuracy of our method. These issues will be addressed in our follow-up work to improve further.

Acknowledgments

Foundation Item: Zigong Key Science and Technology Program (2021QYCX07); Supported by The Innovation Fund of Postgraduate, Sichuan University of Science & Engineering (y2021084).

References

[1] Sun B, Li B. A rapid method to achieve aero-engine blade form detection[J]. Sensors, 2015, 15(6): 12782-12801.

[2] Li D, Li Y, Xie Q, et al. Tiny defect detection in high-resolution aero-engine blade images via a coarse-to-fine framework[J]. IEEE Transactions on Instrumentation and Measurement, 2021, 70: 1-12.

[3] Golnabi H, Asadpour A. Design and application of industrial machine vision systems[J]. Robotics and Computer-Integrated Manufacturing, 2007, 23(6): 630-637.

[4] Zhao Yuanyuan. Application of Computer-based Machine Vision Measurement System in Industrial On-line Detection[J]. Journal of Physics: Conference Series,2021,1992(2).

[5] Ngo N V, Hsu Q C, Hsiao W L, et al. Development of a simple three-dimensional machine-vision measurement system for in-process mechanical parts[J]. Advances in Mechanical Engineering, 2017, 9(10): 1687814017717183.

[6] Huang J, Qi M, Wang Z, et al. High precision measurement for the chamfered hole radius and spacing of a large-size workpiece based on binocular vision combined with plane dynamic adjustment[J]. Applied Optics, 2021, 60(29): 9232-9240.

ISSN: 2414-1895 DOI: 10.6919/ICJE.202301_9(1).0006

[7] Jia L. Research on Key Dimension Detection Algorithm of Auto Parts Based on Hough Transformation [C]//Proceedings of the 2019 International Conference on Robotics, Intelligent Control and Artificial Intelligence. 2019: 184-188.

[8] Canny J. A computational approach to edge detection[J]. IEEE Transactions on pattern analysis and machine intelligence, 1986 (6): 679-698.

[9] Meng Y, Zhang Z, Yin H, et al. Automatic detection of particle size distribution by image analysis based on local adaptive canny edge detection and modified circular Hough transform[J]. Micron, 2018, 106: 34-41.

[10] Gavaskar R G, Chaudhury K N. Fast adaptive bilateral filtering[J]. IEEE Transactions on Image Processing, 2018, 28(2): 779-790.

[11] Gavin H P. The Levenberg-Marquardt algorithm for nonlinear least squares curve-fitting problems[J]. Department of Civil and Environmental Engineering, Duke University, 2019, 19.

[12] Barbosa W O, Vieira A W. On the improvement of multiple circles detection from images using hough transform[J]. TEMA (São Carlos), 2019, 20: 331-342.